Modeling the Dynamics of Wireless Power Transfer Using a Generalized Average Model of High-*Q* Resonators

Hongchang Li[1], Jingyang Fang[2], Xiaoqiang Li[2], Shuxin Chen[2], and Yi Tang[2]
[1]Energy Research Institute, [2]School of Electrical and Electronics Engineering
Nanyang Technological University
Singapore
hongchangli@ntu.edu.sg, yitang@ntu.edu.sg

***Abstract*—Modeling the dynamics of wireless power transfer (WPT) is required by the dynamical control of WPT systems. However, conventional modeling methods for the dynamics of WPT suffer from the order increase problem and complicated derivations and expressions. This paper proposes a much simpler modeling method by using a generalized average model of high-*Q* resonators, which are common components in WPT systems. The proposed method can be easily adopted in systems with various topologies. A pulse density modulated WPT system is modeled as an example. The derived system model includes not only the resonant tanks but also the power converters, and is expressed by a lower order model with more concise formulae as compared to existing dynamical models.**

Keywords—dynamical model; resonator; wireless power transfer (WPT)

I. Introduction

A promising application of wireless power transfer (WPT) is the dynamic charging of online electric vehicles (EVs) [1, 2]. In this application, the coupling coefficient between a transmitter and a receiver changes quickly since online EVs are in motion. Therefore, the dynamical control problem of WPT systems must be resolved. The first step of resolving this problem is modeling the dynamics of WPT.

The difficulties of the modeling come from the complex resonant tanks and power converters in a WPT system. The conventional state-space averaging method for non-resonant converters such as Buck converters is no longer applicable. Generalized state-space averaging (GSSA) and extended describing functions (EDF) are two well-known and effective modeling methods but they increase the order of the model as compared with the number of energy storage elements [3-8]. For example, the WPT system in [6] has 4 resonant elements and 1 filter element, and the order of the model developed in [6] is 9. The modeling method based on coupled modes [9, 10] does not increase the model's order, however, its physical meaning is not straightforward and the derivation processes and expressions are too complicated.

This paper inherits the physical concept in [9, 10] but significantly simplifies the derivation processes and expressions by proposing a generalized average model of high-*Q* resonators in a very concise formula. The resonator model is then applied in a pulse density modulated WPT system as an example.

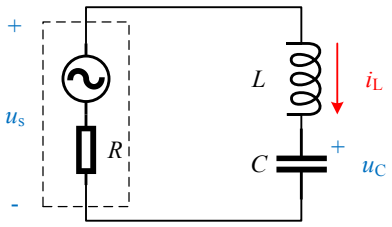

Fig. 1. Resonator driven by a voltage source with an internal resistance.

II. Generalized Average Model of High-*Q* Resonators

Fig. 1 shows an *LC* resonator driven by a voltage source with an internal resistance *R*. The instantaneous driving port voltage is denoted by $u_s(t)$. The instantaneous resonant current and voltage are $i_L(t)$ and $u_C(t)$, respectively. The instantaneous time domain differential equations of the resonator are

$$\begin{cases} \dfrac{\mathrm{d}i_L(t)}{\mathrm{d}t} = -\dfrac{u_C(t)}{L} + \dfrac{u_s(t)}{L} \\ \dfrac{\mathrm{d}u_C(t)}{\mathrm{d}t} = \dfrac{i_L(t)}{C} \end{cases}. \tag{1}$$

The quality factor *Q* is expressed as

$$Q = \frac{\omega L}{R} \tag{2}$$

where ω is a constant reference frequency, which is equal or close to the resonant frequency ω_r, i.e.

$$\omega \approx \omega_r = \frac{1}{\sqrt{LC}}. \tag{3}$$

When *Q* is high and the source frequency ω_s is equal or close to ω, $u_s(t)$, $i_L(t)$, and $u_C(t)$ can be mapped to the slow-varying dynamic phasors $U_s(t)$, $I_L(t)$, and $U_C(t)$, respectively, by

$$\begin{cases} u_{\mathrm{s}}(t)=\mathrm{Re}\left[\sqrt{2}U_{\mathrm{s}}(t)\mathrm{e}^{\mathrm{j}\omega t}\right] \\ i_{\mathrm{L}}(t)=\mathrm{Re}\left[\sqrt{2}I_{\mathrm{L}}(t)\mathrm{e}^{\mathrm{j}\omega t}\right] \\ u_{\mathrm{C}}(t)=\mathrm{Re}\left[\sqrt{2}U_{\mathrm{C}}(t)\mathrm{e}^{\mathrm{j}\omega t}\right] \end{cases}. \tag{4}$$

Since $U_{\mathrm{s}}(t)$, $I_{\mathrm{L}}(t)$, and $U_{\mathrm{C}}(t)$ vary slowly relative to ω, there are

$$\begin{cases} U_{\mathrm{s}}\left(t-\dfrac{\pi}{2\omega}\right)\approx U_{\mathrm{s}}(t) \\ I_{\mathrm{L}}\left(t-\dfrac{\pi}{2\omega}\right)\approx I_{\mathrm{L}}(t) \\ U_{\mathrm{C}}\left(t-\dfrac{\pi}{2\omega}\right)\approx U_{\mathrm{C}}(t) \end{cases}. \tag{5}$$

Therefore, (4) can be approximated to

$$\begin{cases} u_{\mathrm{s}}\left(t-\dfrac{\pi}{2\omega}\right)=\mathrm{Im}\left[\sqrt{2}U_{\mathrm{s}}(t)\mathrm{e}^{\mathrm{j}\omega t}\right] \\ i_{\mathrm{L}}\left(t-\dfrac{\pi}{2\omega}\right)=\mathrm{Im}\left[\sqrt{2}I_{\mathrm{L}}(t)\mathrm{e}^{\mathrm{j}\omega t}\right] \\ u_{\mathrm{C}}\left(t-\dfrac{\pi}{2\omega}\right)=\mathrm{Im}\left[\sqrt{2}U_{\mathrm{C}}(t)\mathrm{e}^{\mathrm{j}\omega t}\right] \end{cases}. \tag{6}$$

Substituting (4) and (6) into (1) and utilizing the linearity and time-invariance of (1), it yields

$$\begin{cases} \dfrac{\mathrm{d}I_{\mathrm{L}}(t)}{\mathrm{d}t}=-\mathrm{j}\omega I_{\mathrm{L}}(t)-\dfrac{U_{\mathrm{C}}(t)}{L}+\dfrac{U_{\mathrm{s}}(t)}{L} \\ \dfrac{\mathrm{d}U_{\mathrm{C}}(t)}{\mathrm{d}t}=-\mathrm{j}\omega U_{\mathrm{C}}(t)+\dfrac{I_{\mathrm{L}}(t)}{C} \end{cases}. \tag{7}$$

The transfer function from $U_{\mathrm{s}}(t)$ to $I_{\mathrm{L}}(t)$ can be derived from (7) based on the linearity and expressed as

$$\frac{I_{\mathrm{L}}(s)}{U_{\mathrm{s}}(s)}=\frac{s+\mathrm{j}\omega}{L\left(s+\mathrm{j}\omega+\mathrm{j}\omega_{\mathrm{r}}\right)\left(s+\mathrm{j}\omega-\mathrm{j}\omega_{\mathrm{r}}\right)}. \tag{8}$$

Considering that the valid frequency range of (8) is much lower than ω, i.e.

$$|s|\ll\omega \tag{9}$$

equation (8) can be approximated to

$$\frac{I_{\mathrm{L}}(s)}{U_{\mathrm{s}}(s)}=\frac{\omega}{L\left(\omega+\omega_{\mathrm{r}}\right)\left(s+\mathrm{j}\omega-\mathrm{j}\omega_{\mathrm{r}}\right)}. \tag{10}$$

Let

$$\begin{cases} \Delta\omega=\omega_{\mathrm{r}}-\omega \\ L_{\omega}=\dfrac{\omega_{\mathrm{r}}+\omega}{\omega}L \end{cases} \tag{11}$$

and transform (10) back into time domain, the generalized average model of the high-Q resonator is obtained:

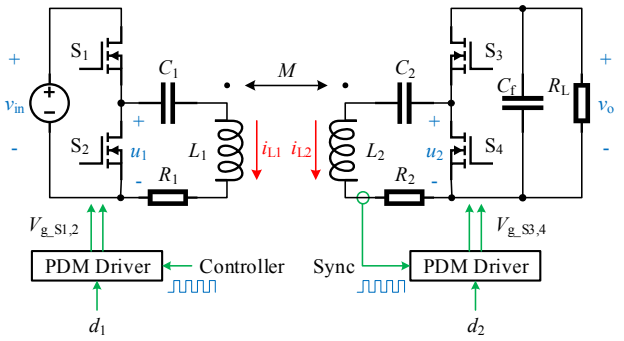

Fig. 2. Pulse density modulated WPT system [11].

$$\frac{\mathrm{d}I_{\mathrm{L}}(t)}{\mathrm{d}t}=\mathrm{j}\Delta\omega I_{\mathrm{L}}(t)+\frac{U_{\mathrm{s}}(t)}{L_{\omega}}. \tag{12}$$

Model (12) is a 1st order linear time-invariant large signal model with complex coefficients and variables. This model can be widely used for various topologies because high-Q resonators are common components in WPT systems.

III. Modeling a Pulse Density Modulated WPT System

As an example, this section models a pulse density modulated WPT system [11], as shown in Fig. 2, where the transmitting side resonator (L_1 and C_1) is driven by a half-bridge inverter and the receiving side resonator (L_2 and C_2) feeds a load R_{L} through a half-bridge rectifier and a filter capacitor C_{f}. M is the mutual inductance between the two sides. R_1 and R_2 are the equivalent series resistances (ESRs). The instantaneous resonant currents of the two resonators are denoted by $i_{\mathrm{L1}}(t)$ and $i_{\mathrm{L2}}(t)$. The instantaneous dc and ac sides voltages of the inverter are $v_{\mathrm{in}}(t)$ and $u_1(t)$, respectively. The instantaneous ac and dc sides voltages of the rectifier are $u_2(t)$ and $v_{\mathrm{o}}(t)$, respectively. The pulse densities of $u_1(t)$ and $u_2(t)$ are $d_1(t)$ and $d_2(t)$, respectively. $d_1(t)$ and $d_2(t)$ are two control degrees of freedom of the system.

The driving sources of the transmitting side resonator include: 1) the voltage drop on R_1, 2) the electromotive force induced by $i_{\mathrm{L2}}(t)$, and 3) $u_1(t)$. The sum of these sources in dynamic phasor domain is

$$\begin{aligned} U_{\mathrm{s1}}(t)=&-R_1I_{\mathrm{L1}}(t)-\mathrm{j}\omega_{\mathrm{s}}MI_{\mathrm{L2}}(t) \\ &+\frac{\sqrt{2}}{\pi}d_1(t)v_{\mathrm{in}}(t)\mathrm{e}^{-\mathrm{j}\gamma\mathrm{sgn}[\arg I_{\mathrm{L1}}(t)]} \end{aligned} \tag{13}$$

where $I_{\mathrm{L1}}(t)$ is the dynamic phasor of $i_{\mathrm{L1}}(t)$, ω_{s} is the angular source frequency of the inverter's modulator, and $\gamma=\omega_{\mathrm{s}}T_{\mathrm{d}}/2$ is the angle that corresponds to half of the inverter's dead time T_{d}.

The driving sources of the receiving side resonator include: 1) the voltage drop on R_2, 2) the electromotive force induced by $i_{\mathrm{L1}}(t)$, and 3) $u_2(t)$. The sum of these sources in dynamic phasor domain is

$$\begin{aligned} U_{\mathrm{s2}}(t)=&-R_2I_{\mathrm{L2}}(t)-\mathrm{j}\omega_{\mathrm{s}}MI_{\mathrm{L1}}(t) \\ &+\frac{\sqrt{2}}{\pi}d_2(t)v_{\mathrm{o}}(t)\mathrm{e}^{\mathrm{j}[\arg I_{\mathrm{L2}}(t)+\pi-\alpha]} \end{aligned} \tag{14}$$

where $I_{L2}(t)$ is the dynamic phasor of $i_{L2}(t)$, and α is a constant synchronization angle for soft switching [11].

In addition, the dynamic of C_f is described by

$$C_f \frac{dv_o(t)}{dt} = \frac{\sqrt{2}\cos\alpha}{\pi} d_2(t)\left|I_{L2}(t)\right| - \frac{v_o(t)}{R_L}. \quad (15)$$

By substituting (13) and (14) into (12) and combining with (15), the average model of the WPT system is obtained:

$$\begin{cases} \dfrac{dI_{L1}(t)}{dt} = j\Delta\omega_1 I_{L1}(t) - \dfrac{R_1}{L_{\omega1}} I_{L1}(t) - \dfrac{j\omega_s M}{L_{\omega1}} I_{L2}(t) \\ \qquad + \dfrac{\sqrt{2}}{\pi L_{\omega1}} d_1(t) v_{in}(t) e^{-j\gamma \mathrm{sgn}[\arg I_{L1}(t)]} \\ \dfrac{dI_{L2}(t)}{dt} = j\Delta\omega_2 I_{L2}(t) - \dfrac{R_2}{L_{\omega2}} I_{L2}(t) - \dfrac{j\omega_s M}{L_{\omega2}} I_{L1}(t) \\ \qquad + \dfrac{\sqrt{2}}{\pi L_{\omega2}} d_2(t) v_o(t) e^{j[\arg I_{L2}(t)+\pi-\alpha]} \\ \dfrac{dv_o(t)}{dt} = \dfrac{\sqrt{2}\cos\alpha}{\pi C_f} d_2(t)\left|I_{L2}(t)\right| - \dfrac{1}{R_L C_f} v_o(t) \end{cases} \quad (16)$$

where ω_s is taken as the reference frequency, ω_1 and ω_2 are the resonant frequencies of the two resonators, respectively,

$$\begin{cases} \Delta\omega_1 = \omega_{r1} - \omega_s \\ L_{\omega1} = \dfrac{\omega_{r1} + \omega_s}{\omega_s} L_1 \end{cases} \quad (17)$$

and

$$\begin{cases} \Delta\omega_2 = \omega_{r2} - \omega_s \\ L_{\omega2} = \dfrac{\omega_{r2} + \omega_s}{\omega_s} L_2 \end{cases}. \quad (18)$$

Model (16) is a 3rd order nonlinear time-invariant large signal model with complex coefficients and variables. The model is continuous at the points where $\arg I_{L1} \neq 0$. A step length of $2\pi/\omega_s$ is sufficient to solve the model.

IV. Experimental Verification

The experimental prototype was built as per Fig. 2. The coils, caps, inverter and rectifier were described in [11]. The coils were co-axially aligned and the face-to-face distance was 0.45 m, as shown in Fig. 3. The parameters of the experimental prototype are listed in Table I.

Model (16) is verified by investigating the system's step responses when stepping the pulse densities d_1 and d_2 between 0.5 and 1. The captured experimental waveforms are shown in Fig. 4. For comparison, Fig. 5 shows the waveforms predicted by model (16), as well as the experimental waveform data.

As can be seen from Fig. 5, the predictions given by (16) coincide very well with the experimental results, indicating that the modeling method based on the average model of high-Q resonators is practicable.

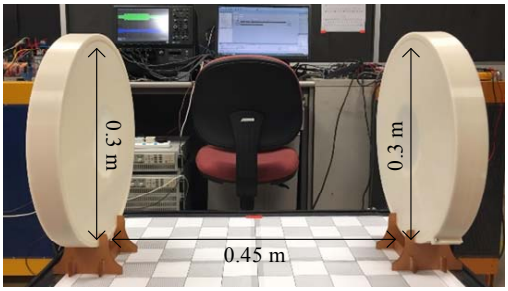

Fig. 3. Alignment of the coils.

TABLE I Parameters of the Experimental Prototype

Symbol	Quantity	Value
V_{in}	Input voltage	29.5 V
f_s	Source frequency	0.909 MHz
T_{d1}	Inverter dead time	50 ns
L_1	Transmitting side resonant inductance	76.7 μH
C_1	Transmitting side resonant capacitance	400 pF
R_1	Transmitting side ESR	1 Ω
M	Mutual inductance	0.96 μH
L_2	Receiving side resonant inductance	76.8 μH
C_2	Receiving side resonant capacitance	400 pF
R_2	Receiving side ESR	1 Ω
α	Synchronization angle	0.51 rad
C_f	Filter capacitance	1 μF
R_L	Load resistance	95 Ω

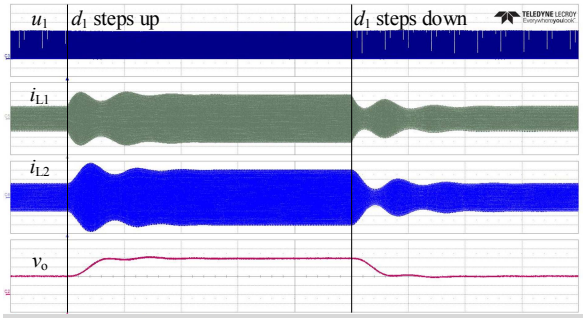

(a)

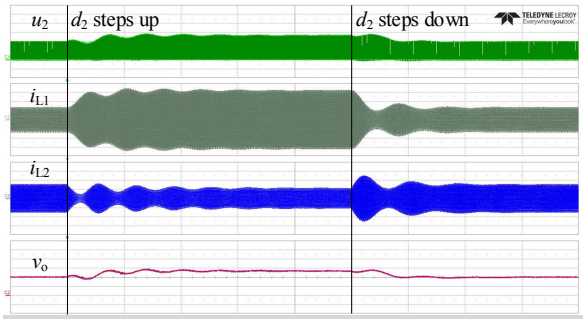

(b)

Fig. 4. Experimental waveforms of the step responses. (a) $d_2 = 0.5$, d_1 steps up to 1 and down to 0.5, (b) $d_1 = 0.5$, d_2 steps up to 1 and down to 0.5.

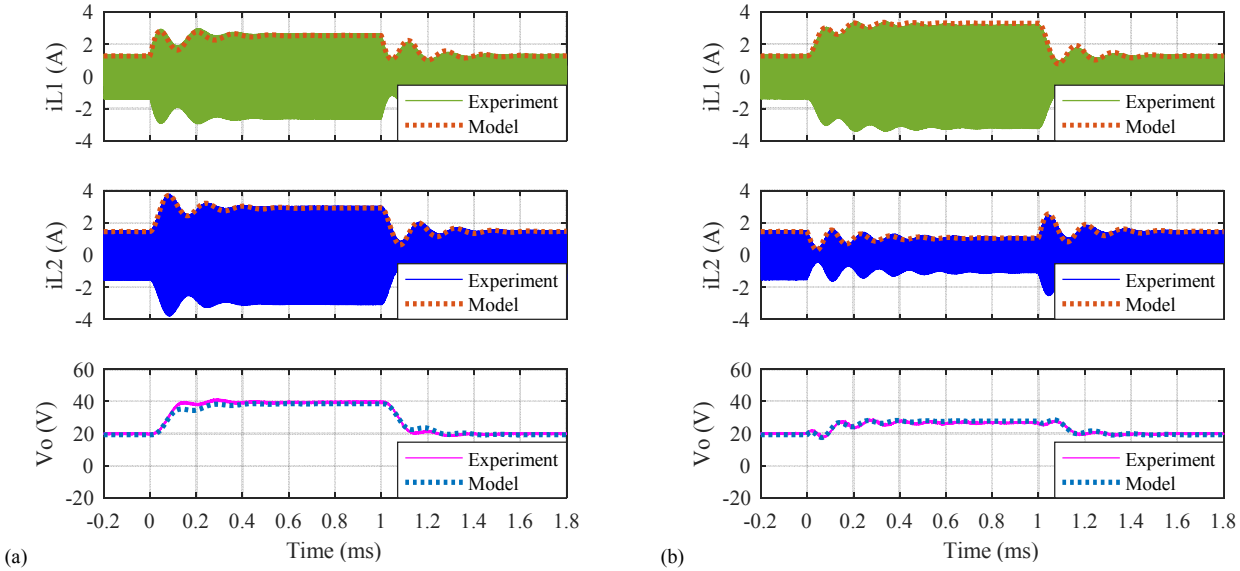

Fig. 5. Experimental data vs. model predictions. (a) $d_2 = 0.5$, d_1 steps up to 1 and down to 0.5, (b) $d_1 = 0.5$, d_2 steps up to 1 and down to 0.5.

V. Conclusion

This paper proposes a 1st order generalized average model for high-*Q* resonators, which are common components in WPT systems. The resonator model is applied in the dynamical modeling of a pulse density modulated WPT system, which has 4 resonant elements and 1 filter element. A 3rd order average model is developed for the system. The accuracy of the model is verified by investigating the system's step responses when the pulse densities step up and down. The model developed in this paper has a much lower order and more concise formulae as compared with the models developed by other methods.

References

[1] C. C. Mi, G. Buja, S. Y. Choi, and C. T. Rim, "Modern Advances in Wireless Power Transfer Systems for Roadway Powered Electric Vehicles," *IEEE Transactions on Industrial Electronics*, vol. 63, pp. 6533-6545, 2016.

[2] J. M. Miller, P. T. Jones, J. M. Li, and O. C. Onar, "ORNL Experience and Challenges Facing Dynamic Wireless Power Charging of EV's," *IEEE Circuits and Systems Magazine*, vol. 15, pp. 40-53, 2015.

[3] A. P. Hu, "Modeling a contactless power supply using GSSA method," in *2009 IEEE International Conference on Industrial Technology*, 2009, pp. 1-6.

[4] H. Hao, G. A. Covic, and J. T. Boys, "An Approximate Dynamic Model of LCL-T-Based Inductive Power Transfer Power Supplies," *IEEE Transactions on Power Electronics*, vol. 29, pp. 5554-5567, Oct 2014.

[5] Z. Huang, S. C. Wong, and C. K. Tse, "Control Design for Optimizing Efficiency in Inductive Power Transfer Systems," *IEEE Transactions on Power Electronics*, 2017. (Published online.)

[6] Z. U. Zahid, Z. Dalala, and J. S. J. Lai, "Small-signal modeling of series-series compensated induction power transfer system," in *2014 IEEE Applied Power Electronics Conference and Exposition (APEC)*, 2014, pp. 2847-2853.

[7] Z. U. Zahid, Z. M. Dalala, C. Zheng, R. Chen, W. E. Faraci, J. S. Lai, et al., "Modeling and Control of Series-Series Compensated Inductive Power Transfer System," *IEEE Journal of Emerging and Selected Topics in Power Electronics*, vol. 3, pp. 111-123, Mar 2015.

[8] H. Feng, T. Cai, S. Duan, X. Zhang, and H. Hu, "Modeling and analysis of phase-shift controlled LCL resonant converter in wireless charging systems," in *2017 IEEE Applied Power Electronics Conference and Exposition (APEC)*, 2017, pp. 3714-3719.

[9] H. Li, J. Li, L. Huang, K. Wang, and X. Yang, "A novel dynamic modeling method for wireless power transfer systems," in *2015 IEEE Applied Power Electronics Conference and Exposition (APEC)*, 2015, pp. 2740-2743.

[10] H. Li, K. Wang, L. Huang, W. Chen, and X. Yang, "Dynamic Modeling Based on Coupled Modes for Wireless Power Transfer Systems," *IEEE Transactions on Power Electronics*, vol. 30, pp. 6245-6253, Nov 2015.

[11] H. Li, J. Fang, S. Chen, K. Wang, and Y. Tang, "Pulse Density Modulation for Maximum Efficiency Point Tracking of Wireless Power Transfer Systems," *IEEE Transactions on Power Electronics*, 2017. (Published online.)